Medical Imaging with Deep Learning

PathologyGAN:
Learning deep representations of cancer tissue

Adalberto Claudio Quiros a.claudio-quiros.1@research.gla.ac.uk
Roderick Murray-Smith roderick.murray-smith@glasgow.ac.uk
Ke Yuan ke.yuan@glasgow.ac.uk
University of Glasgow, Computing Science Department

June 26, 2020

Motivation

Cancer and Tissue Imaging

- Cancer is a heterogeneous disease, with complex micro-environments where lymphocytes, stromal, and cancer cells interact with the tissue and blood vessels.
- Although the genomic and transcriptomic diversity in tumors is quite high, phenotype between/within tumor such as cellular behaviours and tumor micro-environments remains poorly understood.

Why generative models?

- Limitation of supervised learning: Expensiveness of data collection and labeling, it cannot provide unknown information about the data.
- A generative model can to identify and reproduce the different types of tissue.
- Disentangled representations can provide further understanding on phenotype diversity between and within tumors.

We start with BigGAN and Relativistic Average Discriminator.

Loss function: The discriminator, and generator loss function are formulated as in Equations 2 and 3, where $\mathbb{P}$ is the distribution of real data, $\mathbb{Q}$ is the distribution for the fake data, and $C(x)$ is the non-transformed discriminator output or critic:

$$L_{Dis} = -\mathbb{E}_{x_r \sim \mathbb{P}} \left[\log \left(\tilde{D} \left(x_r \right) \right) \right] - \mathbb{E}_{x_f \sim \mathbb{Q}} \left[\log \left(1 - \tilde{D} \left(x_f \right) \right) \right], \tag{1}$$

$$L_{Gen} = -\mathbb{E}_{x_f \sim \mathbb{Q}} \left[\log \left(\tilde{D} \left(x_f \right) \right) \right] - \mathbb{E}_{x_r \sim \mathbb{P}} \left[\log \left(1 - \tilde{D} \left(x_r \right) \right) \right], \tag{2}$$

$$\tilde{D} \left(x_r \right) = \text{sigmoid} \left(C \left(x_r \right) - \mathbb{E}_{x_f \sim \mathbb{Q}} C \left(x_f \right) \right)),$$

$$\tilde{D} \left(x_f \right) = \text{sigmoid} \left(C \left(x_f \right) - \mathbb{E}_{x_r \sim \mathbb{P}} C \left(x_r \right) \right).$$

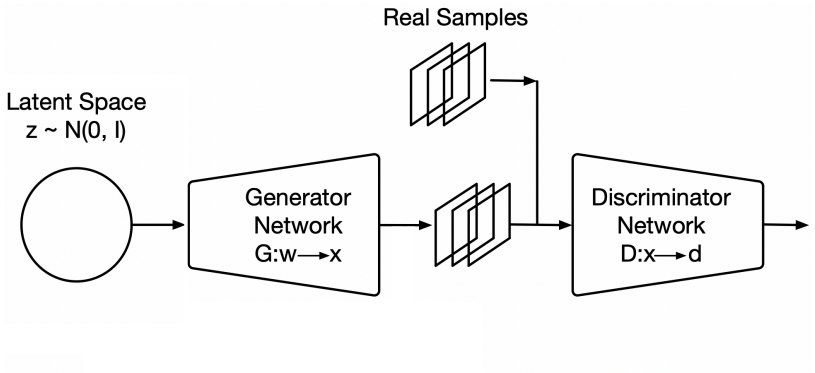

Figure 1: Starting point: BigGAN with Relativistic Average Discriminator.

High quality tissue image generation.

Limitation: No interpretability or structure in the latent space.

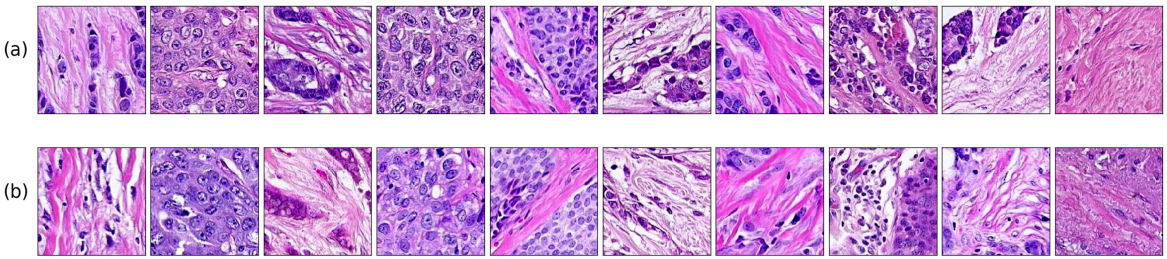

Figure 2: (a): Images (224×224, 448×448) from PathologyGAN trained on H&E breast cancer tissue. (b): Real images, Inception-V1 closest neighbor to the generated above.

Motivation: Can we modify or introduce changes so we have an ordered latent space based on cancer tissue characteristics?

We introduce two features from StyleGAN [1]:

- **Mapping Network [$w \sim M(z)$]:**
  - Neural network that allows to freely optimize the latent space to disentangle high level features in the tissue.
- **Style Mixing Regularization:**
  - To further enforce localize tissue characteristics in the latent space, we use two different latent vectors (z_1, z_2) to generate a single image.
  - We can do this since the latent vector is feed at every level of the generator, we randomly choose a layer in the generator and feed each different latent vector to each half.

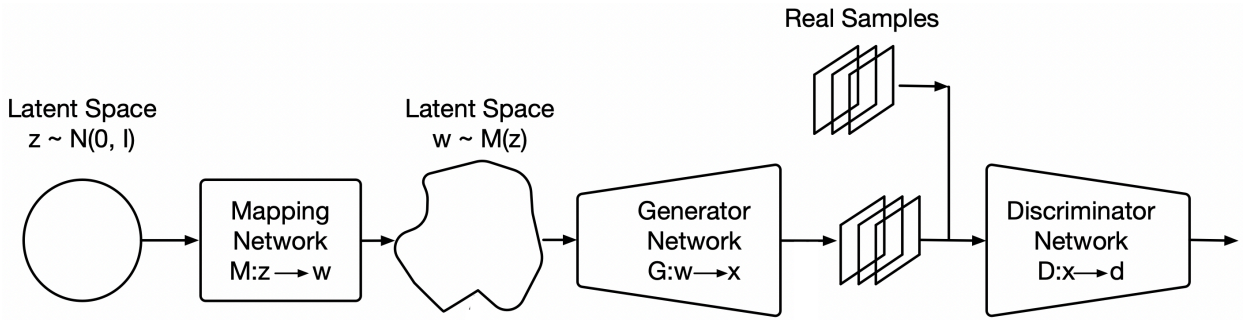

Figure 3: PathologyGAN high level representation

Fréchet Distance: Wasserstein distance between two Gaussians:

We want to measure differences between real and generated tissue distributions.

$$\mathrm{FID} = \left\|\mu_r - \mu_g\right\|^2 + \mathrm{Tr}\left(\Sigma_r + \Sigma_g - 2\left(\Sigma_r \Sigma_g\right)^{1/2}\right);$$
$$\textit{where } X_r \sim \mathcal{N}\left(\mu_r, \Sigma_r\right) \textit{ and } X_g \sim \mathcal{N}\left(\mu_g, \Sigma_g\right)$$

1. *Convolutional Features from an pretrained Inception-V1:* Fréchet Inception Distance (FID).
2. *Cancer tissue characteristics as cancer, lymphocyte, stroma cells count and density:* We use an external tool, CRImage, based on SVM to quantify these in the tissue image.
   - Each image is quantified into a vector: (# cancer cells, # lymph. and stroma, cancer cell density)

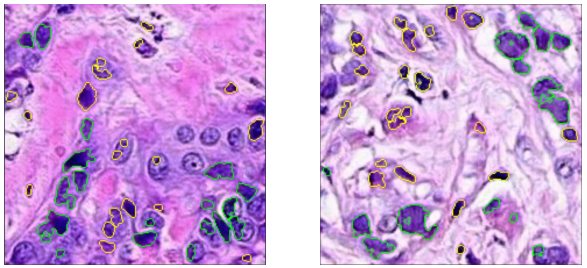

Figure 4: CRImage identifies different cell types in our generated images. Cancer cells are highlighted with a green color, while lymphocytes and stromal cells are highlighted in yellow.

Results - Image Quality

As a reference, values are similar to ImageNet models of BigGAN [2] and SAGAN [3], with FIDs of 7.4 and 18.65 respectively or StyleGAN [1] trained on FFHQ with FID of 4.40:

Model	Inception FID	CRImage FID
PathologyGAN	16.65 ± 2.5	9.86 ± 0.4

Table 1: Evaluation of PathologyGANs. Mean and standard deviations are computed over three different random initializations. The low FID scores in both feature space suggest consistent and accurate representations.

Pathologists' interpretation:

Motivation: Test if experts that work with tissue images find artifacts that give away generated tissue.

1. *Test I:* 25 Sets of 8 images - Pathologists were asked to find the only fake image in each set.
2. *Test II:* 50 Individual images - Pathologists were asked to rate all individual images from 1 to 5, where 5 meant the image appeared the most real.

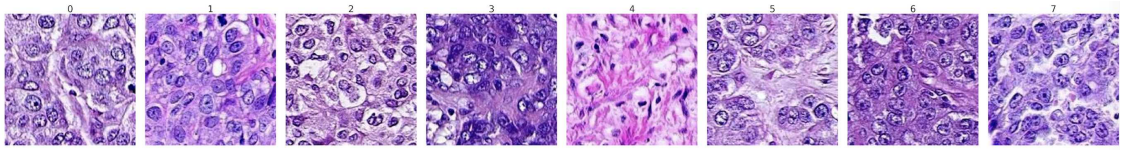

Figure 5: Example of Test I.

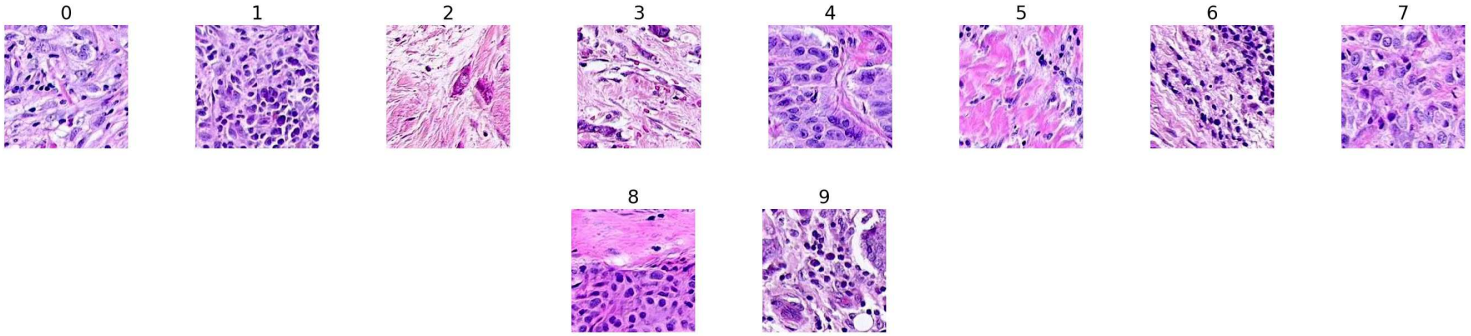

Figure 6: Examples of Test II.

Pathologists' interpretation:

1. *Test I:* Pathologist 1 and 2 were able to find only 2/25 sets and 3/25 fake images.
2. *Test II:* Figure 7 - The near random classification performance from both expert pathologists suggests that generated tissue images do not present artifacts that give away the tissue as generated.

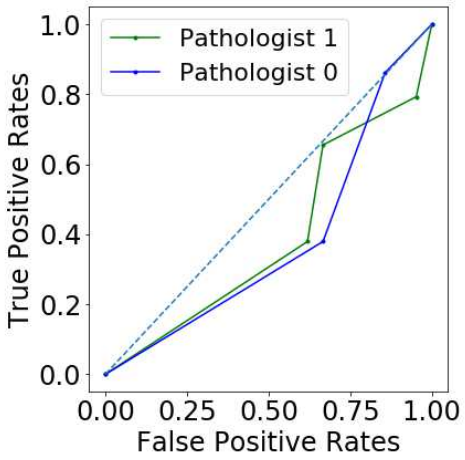

Figure 7: ROC curve of Pathologists' classification for tissue images.

Do we have any kind of structure in the latent space?

1. We generated $10,000$ tissue images, each of them with its associated latent vector $w \in \mathbb{R}^{200}$
2. For each tissue image, we run CRImage to get the count of cancer cells in the tissue.
3. We created 9 different buckets for cancer cell counts. Class 0 accounts for images with the lowest count cancer cells, on the other extreme Class 8 accounts for images with the largest counts.
4. We run UMAP[4] to perform dimensionality reduction from 200 dimensions to 2 dimensions over the complete $10,000$ w lantent vectors.

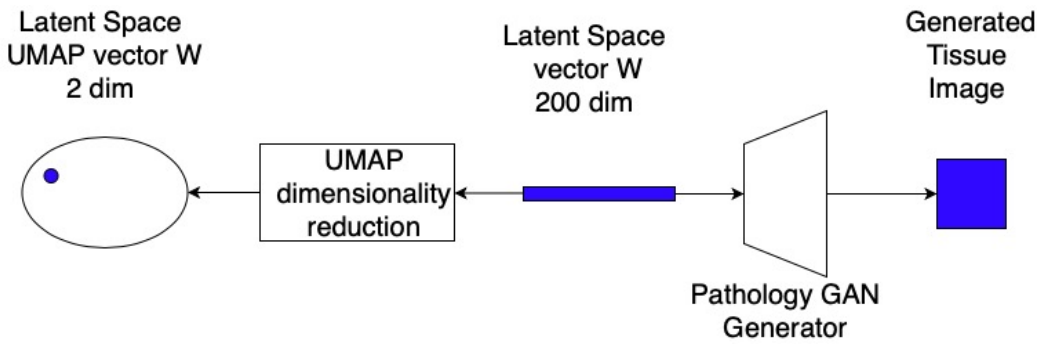

Figure 8: Preprocessing of data for latent space interpreztation.

Difference between PathologyGAN's and BigGAN's latent space:

- (a) PathologyGAN shows structure in the latent space w making the image generation interpretable, increasing counts in cancer cells correspond to moving the selected vector from quadrant IV to quadrant II
- (b) Vector samples are randomly placed in the BigGAN's latent space w.

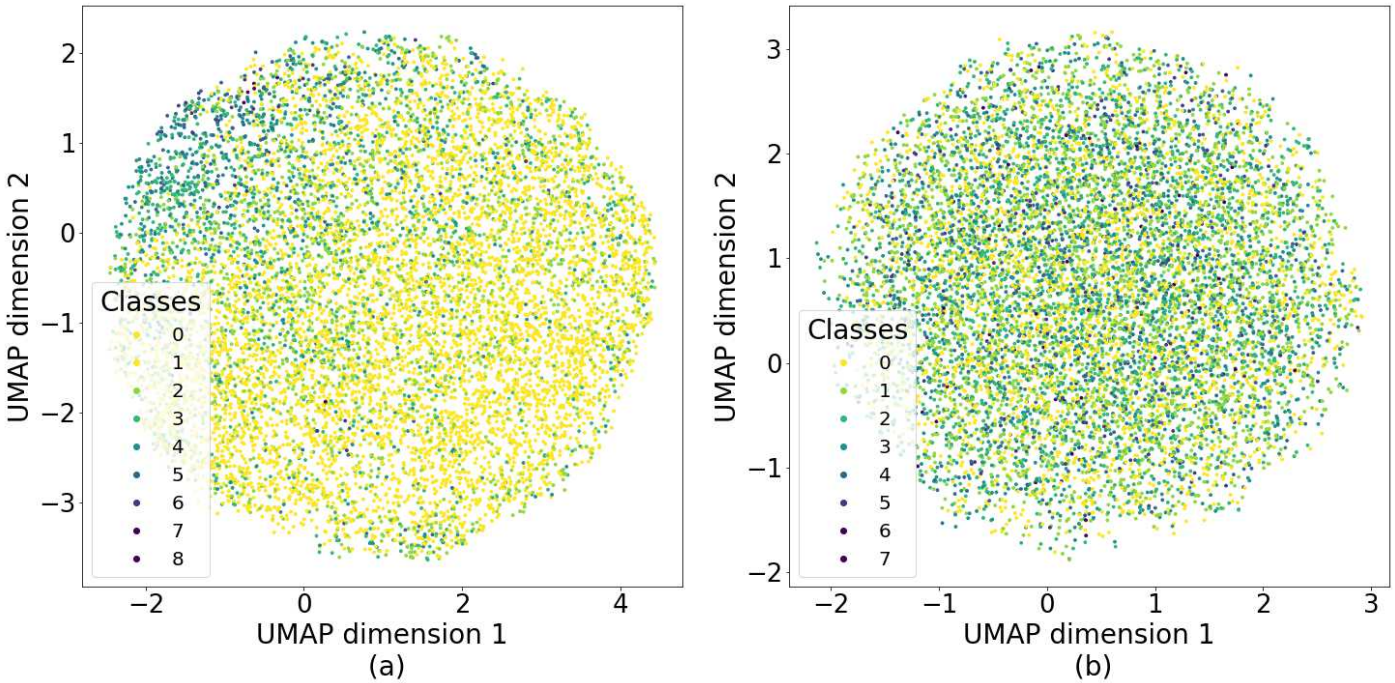

Figure 9: Contrast between PathologyGAN's latent space (a) and BigGAN's (b).

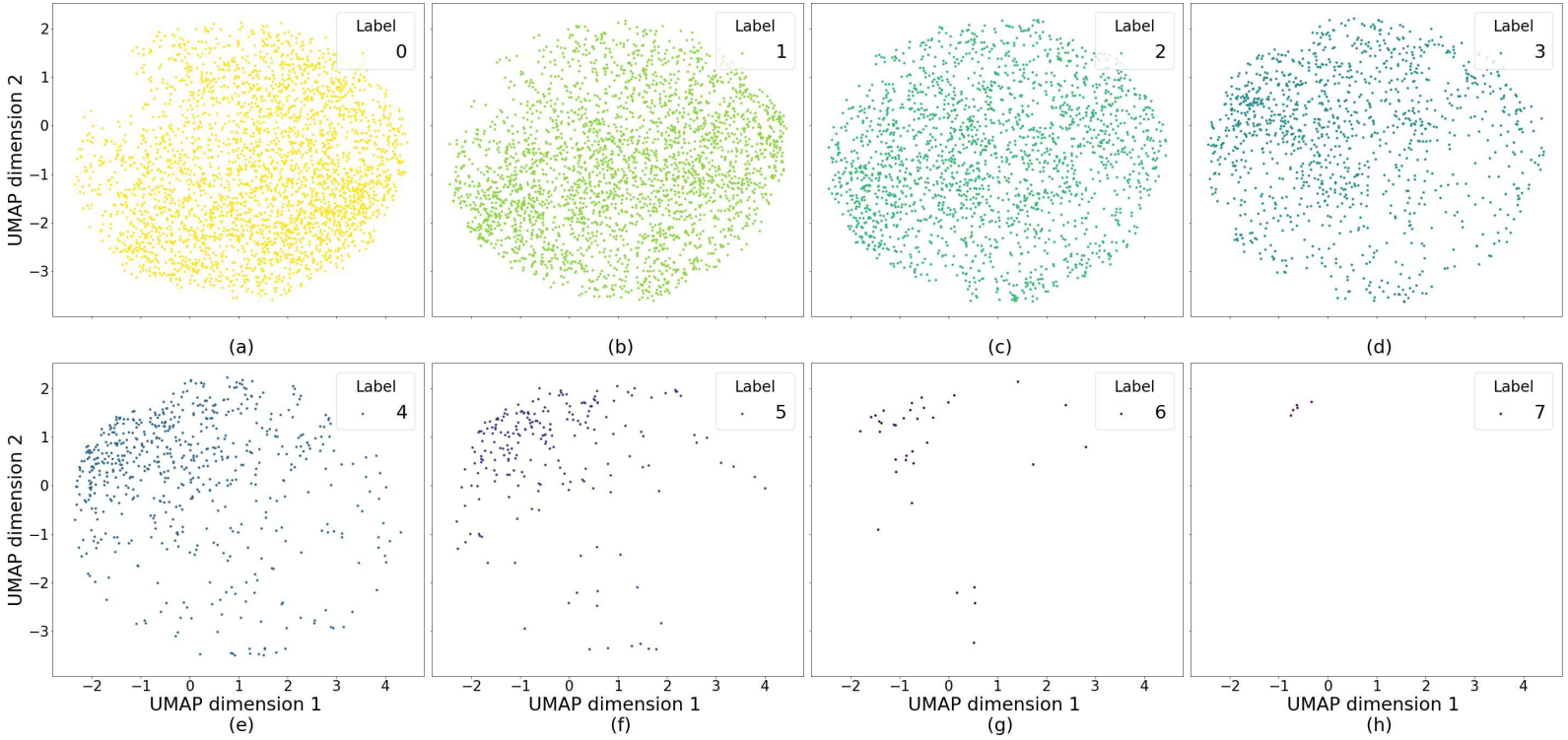

Figure 10: Scatter plots with w latent vectors on PathologyGAN's latent space. Each sub-figure shows datapoints only related to one of the classes, and each class is subject to the count of cancer cells in the tissue image, (a) [class 0] are associated to images with the lowest number of cancer cells, (h) [class 8] with the largest.

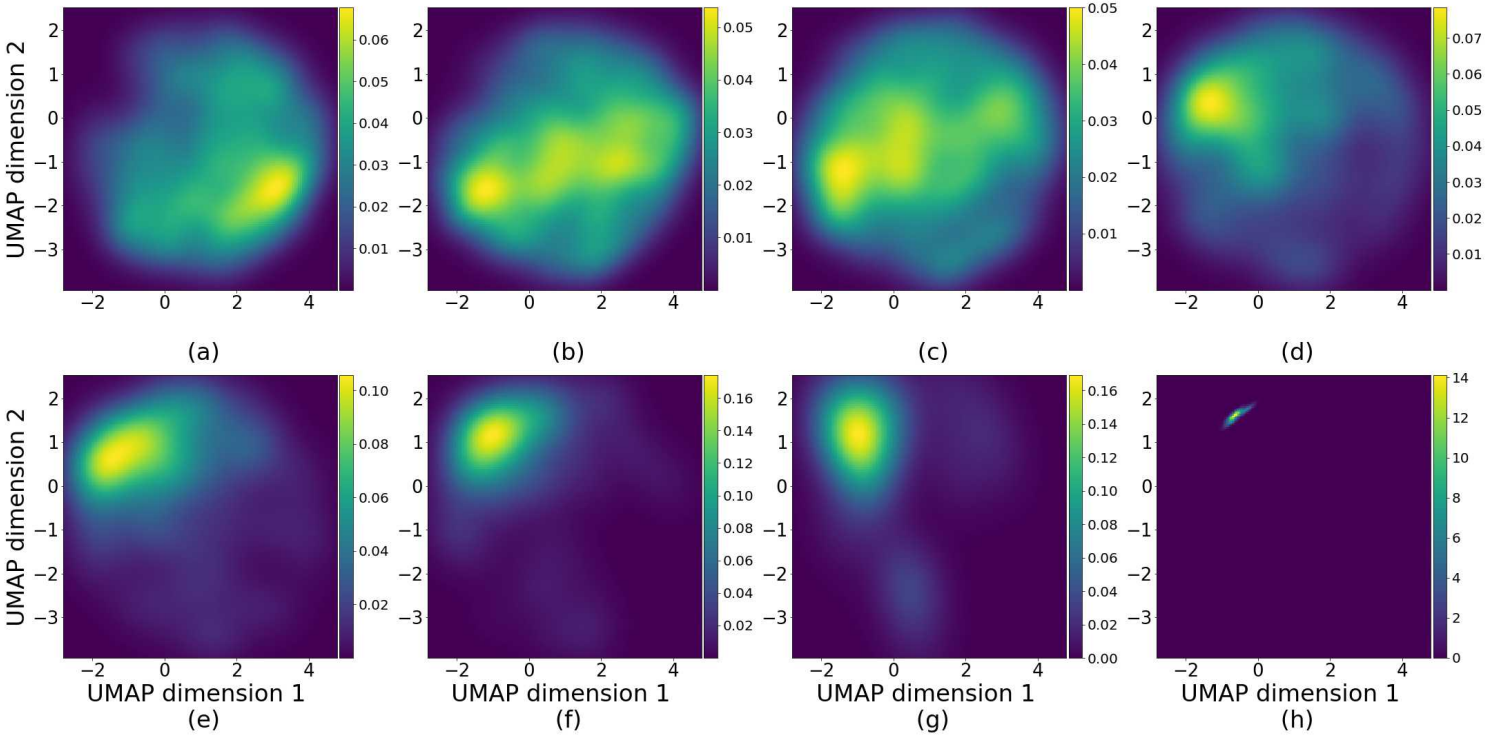

Figure 11: Density plots with w latent vectors on PathologyGAN's latent space. Each sub-figure shows datapoints only related to one of the classes, and each class is subject to the count of cancer cells in the tissue image, (a) [class 0] are associated to images with the lowest number of cancer cells, (h) [class 8] with the largest.

Linear interpolation:

- We captured two latent vectors z with associated tissue: benign (less cancer cells, left end) and malignant tissue (more cancer cells, right end).
- We performed a linear interpolation of 8 stages between these two vectors and fed the generator.

Conclusions:

- PathologyGAN (a) includes an increasing population of cancer cells rather than a fading effect from BigGAN (b).
- PathologyGAN (a) better translates high level features of the images from the latent space vectors.

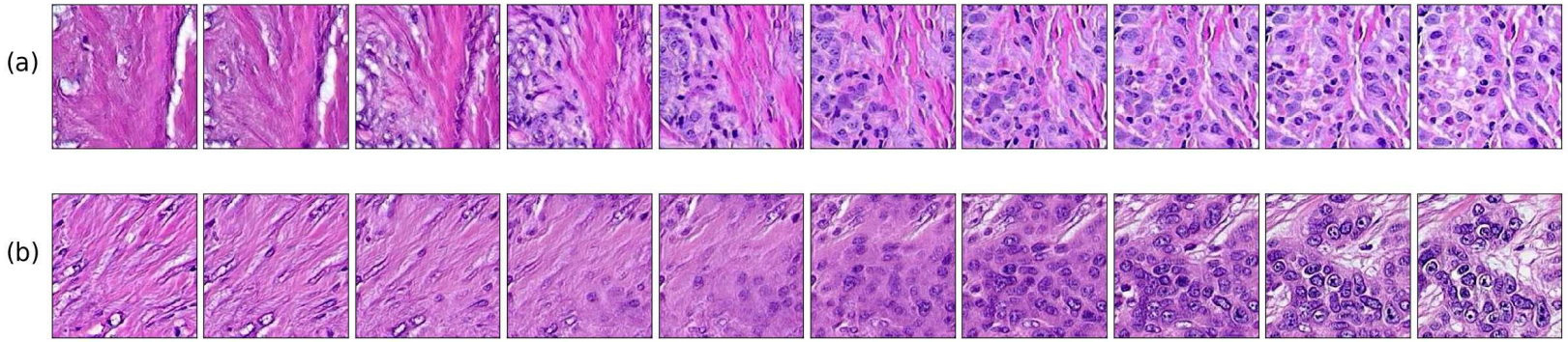

Figure 12: (a) PathologyGAN model. (b) BigGAN model.

Vector Operations:

1. We gather latent vectors z that generate images with different high level features: Benign tissue, lymphocytes, stroma, and tumorous tissue.
2. We performed different linear vector operations before we fed the generator.

Conclusions:

1. The resulting images hold the feature transformations implied in the vector operations.

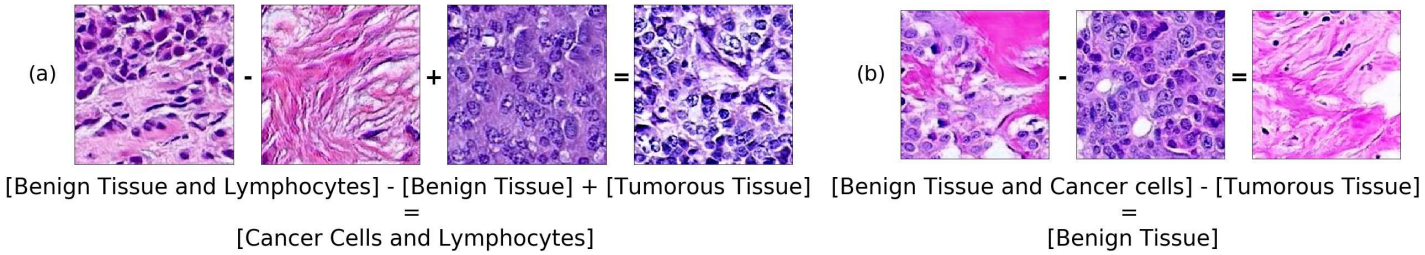

Figure 13: Examples of vector operations.

Acknowledgements

Thanks to Joanne Edwards and Elizabeth Mallon for the helpful insight and discussion on digital pathology.

- Dr. Joanne Edwards - University of Glasgow
- Dr. Elizabeth Mallon - University of Glasgow

Thanks

Thank you for checking out our work!

[1] Tero Karras, Samuli Laine, and Timo Aila.
A style-based generator architecture for generative adversarial networks.
2019 IEEE/CVF Conference on Computer Vision and Pattern Recognition (CVPR), Jun 2019.

[2] Andrew Brock, Jeff Donahue, and Karen Simonyan.
Large scale gan training for high fidelity natural image synthesis, 2018.

[3] Han Zhang, Ian Goodfellow, Dimitris Metaxas, and Augustus Odena.
Self-attention generative adversarial networks, 2018.

[4] Leland McInnes, John Healy, and James Melville.
Umap: Uniform manifold approximation and projection for dimension reduction, 2018.